

Canine Thoracic Radiographs Classification Using Deep Learning Algorithms: An Investigation

Ashendra Kumar Saxena¹, Dr. Divakara Sastry EV², Roopashree³

¹Professor, College of Computing Science and Information Technology, Teerthankar Mahaveer University, Moradabad, Uttar Pradesh, India, Email id- ashendrasaxena@gmail.com

²Professor, School of Agricultural Sciences, Jaipur National University, Jaipur, Rajasthan, India, Email id- evdivakara.sastry@jnujaipur.ac.in

³Assistant Professor, Department of Chemistry, School of Sciences, JAIN (Deemed-to-be University), Karnataka, India, Email Id- r.roopashree@jainuniversity.ac.in

Abstract

Thoracic radiograph interpretation is a difficult and error-prone job for veterinarians. Even with recent developments in machine learning and computer vision, creating computer-aided diagnostic tools for radiographs is still a difficult and unresolved challenge, especially in veterinary medicine. This research aimed to develop a unique approach for categorizing canine thoracic radiographs (CTR) using Enhanced Layer wise deep neural Networks (EL-DNN). Thoracic radiographs of canine patients were collected retrospectively from 2010 to 2020. The radiograph data was split in half because it came from two distinct radiograph acquisition methods. The EL-DNNs' generalizability was evaluated using Data Set 2, whereas Data Set 1 was utilized for training and testing. We built and evaluated two alternative EL-DNNs, one using the ResNet-50 architecture and the other using the DenseNet-121. The area under the Receiver Operator Curve (AUC) values over 0.8 were achieved by the ResNet-50-based EL-DNN for all included radiographic findings on Data Sets 1 and 2, except bronchial and interstitial patterns. The overall performance of the DenseNet-121 EL-DNN was inferior. The EL-DNN trained on ResNet-50 outperformed the other regarding generalization ability, demonstrating superior performance for the alveolar, megaesophagus, interstitial, and pneumothorax.

Keywords: DenseNet-121, ResNet-50, Enhanced Layer wise deep neural Networks (EL-DNN), and canine thoracic radiographs (CTR)

Introduction

A common imaging technique used to assess the anatomy within the thoracic cavity is a thoracic radiograph, commonly known as a chest X-ray. Between the neck and the belly is the thoracic cavity, which houses important organs, including the heart, lungs, and major blood veins. Thoracic radiographs help diagnose various respiratory and cardiac disorders while providing useful information about these structures (1). The patient is normally placed in a standing or reclining posture for thoracic radiography. The X-ray machine emits a regulated amount of radiation, which travels through the patient's body and interacts with the underlying tissues. The interior chest structures are visible in the X-ray picture because different systems attenuate the radiation differently (2, 3). The size and form of the heart may be assessed, and any anomalies such as cardiomegaly (an enlarged heart) or pericardial effusion (fluid around the heart) can be found. The lung fields might be checked for indications of an infection, congestion, tumors, or other clinical problems (4).

Fractures, dislocations, or herniations in the ribs and diaphragm are examined. The presence of masses or nodules in the lungs, which may be a sign of lung cancer or metastatic illness,

may also be seen on thoracic radiographs. The region between the lungs, known as the mediastinum, may also be scrutinized for anomalies, including enlarged lymph nodes, tumors, or fluid accumulations (5). Diagnoses of respiratory disorders, including pneumonia, pneumothorax (collapsed lung), pulmonary edoema (fluid in the lungs), and chronic obstructive pulmonary disease (COPD), may all be made using thoracic radiography. They may assist in determining the underlying reason for patients' recurrent coughing or respiratory discomfort (6, 7). Thoracic radiographs are very important in the diagnosis of heart abnormalities in addition to respiratory disorders. Among the diseases they could identify are congenital cardiac defects, valve disease, and congestive heart failure. It is possible to gauge the size of the heart chambers and the condition of the blood vessels, providing vital diagnostic information that can help guide future treatment (8). A good diagnostic method for figuring out what's in the thoracic cavity is taking thoracic radiographs. They assist in diagnosing several diseases that may impair the heart, lungs, and other organs early. These radiographs need to be read by a professional, and they are often combined with other diagnostic procedures to provide a full assessment of the patient's health (9). In veterinary medicine, canine thoracic radiographs are a crucial diagnostic tool for determining the health and condition of a dog's chest cavity. These radiographs precisely visualize many thoracic organs and tissues, including the heart, lungs, trachea, and ribs. They are often carried out to assess breathing issues, find anomalies, track the evolution of illnesses, and help diagnose different disorders (10, 11). The method involves placing the dog on its side or back while many X-ray images are obtained from various angles. To guarantee optimal placement to reduce tension or movement, which might influence the quality of the images, the dog might need to be tranquilized or immobilized. Protective lead shielding must be used to prevent the patient and the veterinary team from unnecessarily being exposed to radiation (12, 13). Thoracic radiographs may be a useful tool for more than only detecting particular diseases; they can also provide important details about the dog's general health (14). Canine thoracic radiographs are non-invasive, secure, and reliable imaging methods that are very important in analyzing and conducting different thoracic turmoil in dogs. They help develop suitable treatment strategies for the welfare of canine patients by offering insightful information on the internal workings of the chest (15).

Research (16) evaluated a convolutional neural network (CNN) based computer-aided detection (CAD) device for identifying canine cardiomegaly in standard radiographs. Radiographs taken from the right side of the chest were randomly chosen from the historical record. As a result, veterinarians may soon be able to use convolutional neural networks to aid in diagnosing cardiomegaly in dogs using radiographs. Research (17) aimed to retrospectively apply the deep learning AI approach to thoracic radiographs to identify canine left atrial enlargement and compare the findings to veterinary radiologist interpretations. Research (18) evaluated the viability of using machine learning methods to classify correct cranial and caudal border collimation in ventrodorsal and dorsoventral thoracic radiographs. The Ontario Veterinary College's Picture Archiving and Communication system (PACs) was scoured for 900 radiographs of dogs' and cats' chests taken from both the dorsal and ventral

perspectives. In the summer of 2022, one radiologist categorized the cranial and caudal boundaries of radiographs taken between April 2020 and May 2021 as suitably or incorrectly collimated. A machine learning model was educated to recognize when the cranial and caudal limits of the lung field should be properly included. The combined findings of the cranial and caudal boundary evaluations were used to evaluate both the individual models and a combined overall inclusion model. Thoracic radiographs (TRs) are a common supplementary exam in small animal medicine, but they call for careful interpretation if the RPP is to be utilized to its full potential. The effect on CNN performance of manually segmenting the intrathoracic region of TR and using the boosting contrast approach is compared (19). Clinical applications of artificial intelligence (AI) algorithms in diagnostic imaging are expanding in veterinary medicine. One benefit is that it frees busy radiologists to concentrate on more complicated situations, such as those that arise during an emergency when no board-certified specialist is on staff to interpret the images. This research aimed to examine how well an AI program could identify pleural effusion in canine chest X-rays. Sixty-two canine participants were included in this retrospective, diagnostic case-controlled investigation (20).

Research (21) used historical data to create a novel radiographic indicator based on deep learning for assessing canine heart size. The "adjusted heart volume index" (aHVI) was derived from basic lateral X-rays by multiplying the total heart area and dividing the result by the length. Segmentation and quantitative evaluation are fundamental to the algorithms. Images were hung incorrectly to simulate every potential mistake made in clinical practice, such as horizontal flips and rotation. We obtained radiographic pictures and split them into three distinct groups: training (800), testing (240), and validation (208). The structures' capacity to recognize flips, rotations, and both flips and rotations simultaneously were evaluated (22). Research (23) used the interpretation of a veterinary radiologist certified by the American College of Veterinary Radiology as the gold standard to compare the diagnostic performance of AI-based software for identifying carcinogenic pulmonary edoema in canines from thoracic radiographs. One veterinary hospital's after-hours emergency service radiograph archive was combed for 500 consecutive thoracic images of canines. Beginning with the automation of canine radiographs sorted by view and anatomy, this study delves into these fundamental ideas. While the models built using these deep learning techniques may achieve high levels of accuracy, their insatiable appetite for memory is a drawback that has yet to be adequately addressed. Therefore, this work proposes a new lightweight method that takes cues from AlexNet, Inception, and Squeeze Net (24). Research (25) evaluated an AI-based method for identifying typical technical flaws in canine thoracic radiography. The algorithm aims to determine whether a picture is proper by identifying whether or not it has been rotated, underexposed, overexposed, blurred, cut off, or contains any unwanted items or medical equipment. This research aimed to develop a unique approach for categorizing canine thoracic radiographs (CTR) using Enhanced Layer wise deep neural Networks (EL-DNN).

Materials and Methods

Enhanced Layer wise deep neural Networks (EL-DNN)

An epoch in deep learning refers to a complete iteration across a specific dataset. Errors can be minimized to a significant extent by the use of back propagation to adjust the number of epochs. One method that can be utilized in determining a classification scheme's success is a confusion matrix. In the format of rows and columns, a confusion matrix presents information about the current and anticipated classes. The several network layers of the EL-DNN are divided into different sections.

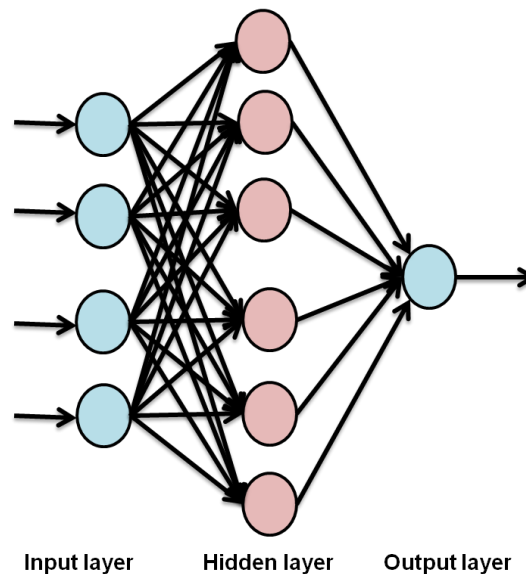


Figure (1): Structure of deep neural networks

Figure 1 illustrates that deep neural networks extract hidden learning from large datasets. Keras is a Python package that allows users to construct and evaluate deep learning models efficiently and flexibly—wrapping two of the most powerful numerical computation libraries currently available, Theano and Tensor Flow, allowing you to easily characterize and develop neural system models using only a few lines of code at the most. Data is received at the top layer, displayed at the bottom, and kept secret at all other layers. The model is run, and the output is gathered. To finish the DNN model training, back propagation is used, though. Or, the loss function quantifies the difference between expected and actual results. The bias B and weight coefficient W continually change throughout the training process.

$$I(V, a, y, x) = \frac{1}{2} \|x^K - x\|_2^2 = \frac{1}{2} \sigma(V^K x^{K-1} + a^K) - x\|_2^2 \quad (1)$$

The buried layer's output is denoted by x^K .

An EL-DNN is a particular kind of artificial neural network (ANN) made up of several layers of nodes that are connected or neurons. It is intended to comprehend intricate patterns and understand hierarchical data structures. The word "deep" describes how many hidden layers exist in the network between the input and output layers.

EL-DNN neurons cooperate to produce outputs by applying an activation function to the inputs from the layer above them. The network may gradually extract more complex characteristics and representations from the input data since each layer's output serves as the input for the layer above it. An EL-DNN hidden layer allows it to model complex connections and detect non-linearities in the data.

Due to its capacity to provide cutting-edge performance in some areas, including computer vision, natural language processing, and voice recognition, deep neural networks have attracted much interest and popularity in recent years.

Back propagation is a technique used in the training of EL-DNN that employs gradient descent optimization to update the weights and biases of the network depending on the calculated error or loss. Large-scale deep neural networks are often trained using methods like stochastic gradient descent (SGD) and regularisation to avoid over fitting and enhance generalization.

Using their capacity to automatically learn complicated representations from raw data, EL-DNN has revolutionized several areas of artificial intelligence, resulting in considerable improvements in many applications.

Database creation

Radiographic findings

Three board-certified veterinary radiologists (AZ, TB, and SB) with a combined twenty, ten, and three years of experience independently examined the pictures. Radiograph exposure and patient location were assessed before interpretation to ensure optimal picture quality. In both collections, we only included well-lit shots where the animal is in the appropriate setting. Images with obvious artifacts and puppy radiographs were also disqualified. Latero-lateral (LL) and ventral (VD) radiographs of the same subject were compared when both were available. Radiographs were categorized only based on the existence or nonexistence of personality radiographic findings rather than on the presence or nonexistence of diseases or states that may be characterized by the concurrent fact of the many conclusions. These radiological abnormalities were used to name all of the images: pleural effusion, pneumothorax, hernia, alveolar pattern, megaesophagus, fracture, interstitial pattern, mass, bronchial pattern, pneumomediastinum, cardiomegaly, tracheal collapse. The image was deemed unremarkable if no abnormalities were seen on the radiograph. Neither the alveolar nor the interstitial pattern's distribution (focal vs. diffused) was considered. Mild, moderate, and severe descriptions were assigned to interstitial and bronchial patterns. Radiographs were deemed nondescript if they showed only minimal bronchial and interstitial patterns. Megaesophagus was given to cases that had both segmental and diffuse changes in the esophagus.

The writers used their expertise to diagnose cardiomegaly. Vertebral heart scores were determined in situations of uncertainty and compared to breed-specific reference intervals found in the published literature. The mass label covered the chest wall and meditative masses as well. Hernias of the diaphragm and the abdominal wall were also included. Rib

fractures and spinal fractures were both categorized as fractures. Long bone fractures were not taken into account. The tracheal collapse did not get any grades. All three writers saw all photographs at the same time, and labels were decided upon after a round of debate.

Image processing and deep learning

A special workstation with four Tesla V100s, an Intel Xeon CPU running at 2.2 GHz, and 256 GB of RAM was used for the deep-learning investigation. Image resolution was reduced to 224x224 before being fed into the EL-DNN. The images were not cropped, less compressed, or converted to JPEG during the testing period. As an alternative, we employed the lossless MHA format. Classification of radiographs was accomplished using two distinct EL-DNN architectures, (1) DenseNet-121 and (2) ResNet-50. EL-DNN is a subset of deep learning algorithms optimized for visual tasks. All EL-DNNs put through their paces had previously been trained on the massive collection of commonplace photos known as ImageNet. A multi-label method was adopted since many radiographic abnormalities are sometimes seen on a single radiograph, typically due to a single ailment. The goal function was the binary cross-entropy. Each network was trained with an identical set of inputs. Using an exponentially decaying scheduler for the learning rate and the Adam optimizer, we introduced until convergence was achieved. The photographs were scaled so zero represents the background and one means the foreground. Data Set 1 was partitioned into training, validation, and test sets with an 8:1:1 split. None of the assessment metrics, such as AUC, sensitivity, or specificity, were explicitly optimized by the training approach. Data Set 2 was not used in any way throughout the learning process.

Statistical analysis

Using widely available statistical software (MedCalc), we compared different topologies by calculating the AUC. Positive likelihood ratio (PLR) = sensitivity / (1 - specificity) and negative likelihood ratio (NLR = (1 - sensitivity)/specificity) were computed. Sensitivity = true positive / (true positive + false negative). The DeLong test was used to compare the two designs' results, but only on Data Set 2.

Results

Database

There were a total of 3839 later-lateral (LL) radiographs in the whole database. There were 3063 LL photos in Data Set 1. However, 632 had to be thrown out because of poor placement or image quality. Despite including 776 LL in Data Set 2, 77 LL radiographs had to be omitted due to placement mistakes or subpar quality. Both databases shared that "unremarkable" and "cardiomegaly" was the most common abnormalities. Radiographic results were not evenly distributed across the 2 data sets; some were over-represented in Data Set 2, while others were under-represented in Data Set 1.

Selection of the radiographic findings

Due to the low sample size in Data Set 1 (Table 1), radiographs depicting tracheal collapse, hernia, pneumomediastinum, and fracture were not included in the training process. Thus, the following radiological diagnoses were utilized to teach the network: normal, bronchial pattern, cardiomegaly, mass, pleural effusion, alveolar pattern, interstitial pattern, pneumothorax, and megaesophagus.

Table (1): Radiographic results from the following number of LL radiography

Radiographic Finding	Dataset 1	Data set 2
Unremarkable	366	1289
Pleural effusion	17	77
Alveolar pattern	42	60
Pneumothorax	13	34
Megaesophagus	22	34
Cardiomegaly	139	584
Bronchial pattern	34	124
Mass	33	95
Hernia	3	6
Fracture	4	6
Excluded	78	633

Classification results

For all other radiographic abnormalities except pleural effusion, ResNet-50 outperformed DenseNet-121 in terms of classification accuracy on both Data set (DS) 1 and DS 2.

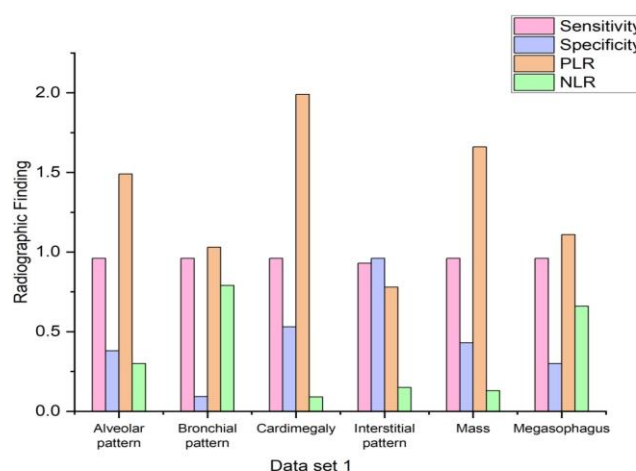


Figure (2): Comparison of ResNet-50 (dataset 1) of radiographic findings

Table (2): Numerical outcomes of ResNet-50 (dataset 1)

DS 1	Radiographic Finding			
	Sensitivity	Specificity	PLR	NLR
Alveolar pattern	0.96	0.38	1.49	0.3
Bronchial pattern	0.96	0.093	1.03	0.79
Cardiomegaly	0.96	0.53	1.99	0.09
Interstitial pattern	0.93	0.96	0.78	0.15
Mass	0.96	0.43	1.66	0.13
Megaesophagus	0.96	0.3	1.11	0.66

Figures 2, 3, and 4 show the results of a classification test conducted on DS 1 and DS 2 using the two designs.

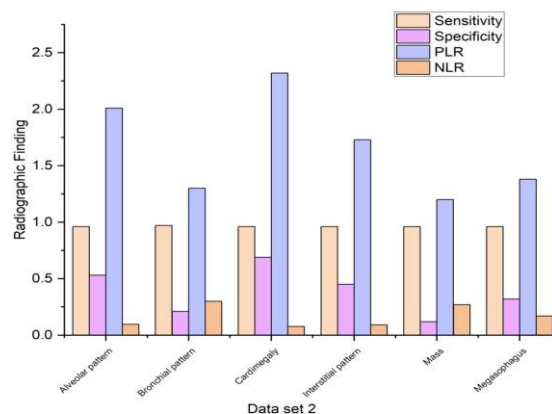


Figure (3): Comparison of ResNet-50 (dataset 2) of radiographic findings

The alveolar pattern is one area where both designs excelled on DS 2, demonstrating more precision than on DS 1. As a result, DenseNet-121 performed better on DS 2 than DS 1 for a variety of conditions, including bronchial pattern, cardiomegaly, megaesophagus, normal, and pneumothorax.

Table (3): Numerical outcomes of ResNet-50 (dataset 2)

DS 2	Radiographic Finding			
	Sensitivity	Specificity	PLR	NLR
Alveolar pattern	0.96	0.53	2.01	0.096
Bronchial pattern	0.97	0.21	1.3	0.3
Cardiomegaly	0.96	0.69	2.32	0.077
Interstitial pattern	0.96	0.45	1.73	0.09

Mass	0.96	0.12	1.2	0.27
Megaesophagus	0.96	0.32	1.38	0.17

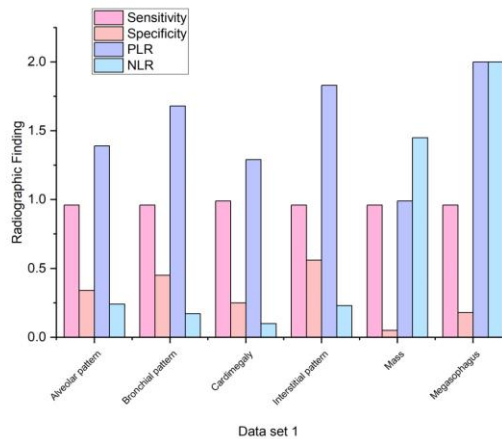


Figure (4): Comparison of DenseNet-121 (dataset 1) of radiographic findings

Table (4): Numerical outcomes of DenseNet-121 (dataset 1)

DS 1	Radiographic Finding			
	Sensitivity	Specificity	PLR	NLR
Alveolar pattern	0.96	0.34	1.39	0.24
Bronchial pattern	0.96	0.45	1.68	0.17
Cardiomegaly	0.99	0.25	1.29	0.1
Interstitial pattern	0.96	0.56	1.83	0.23
Mass	0.96	0.05	0.99	1.45
Megaesophagus	0.96	0.18	2	2

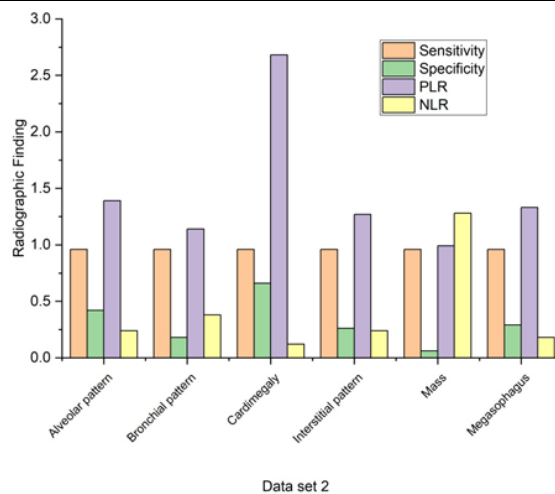


Figure (5): Comparison of DenseNet-121 (dataset 2) of radiographic findings

When compared to DS1, DS 2 accuracy was worse for the other radiographic results. Table 2, 3, 4, and 5 shows the outcomes of ResNet-50 & DenseNet-121 (for dataset 1, 2) for sensitivity, specificity, positive likelihood ratio (PLR), negative likelihood ratio (NLR). Table 6 shows numerical outcomes for AUC.

Table (5): Numerical outcomes of DenseNet-121 (dataset 2)

DS 2	Radiographic Finding			
	Sensitivity	Specificity	PLR	NLR
Alveolar pattern	0.96	0.42	1.39	0.24
Bronchial pattern	0.96	0.18	1.14	0.38
Cardiomegaly	0.96	0.66	2.68	0.12
Interstitial pattern	0.96	0.26	1.27	0.24
Mass	0.96	0.06	0.99	1.28
Megasophagus	0.96	0.29	1.33	0.18

Table 6: Numerical outcomes of DenseNet-121 & ResNet-50

Test set	Radiographic finding	AUC
Data set 1	Aloveolar pattern	0.88
Data set 2	Aloveolar pattern	0.90
Data set 2	Bronchial pattern	0.70
Data set 1	Cardiomegaly	0.93
Data set 2	Cardiomegaly	0.90
Data set 1	Interstitial pattern	0.93
Data set 2	Interstitial pattern	0.80
Data set 1	Mass	0.78
Data set 2	Mass	0.67
Data set 1	Megasophagus	0.79
Data set 2	Megasophagus	0.81

Discussion

A unique deep learning-based EL-DNN is described for automating the detection of several radiographic anomalies in CTR. It seems that multi-label EL-DNNs may be effectively trained even within the situation of moderately miniature-sized & very imbalanced datasets since both evaluated designs demonstrated good classification accuracy on Data Set 2 for practically all the radiography observations. However, it is not always simple to compare veterinary and human medical literature due to discrepancies in categorizing various radiographic findings. Furthermore, radiographic abnormalities like emphysema and fibrosis, which are frequent in humans, are uncommon in dogs. However, for unremarkable radiographic features, including pneumothorax, cardiomegaly, consolidation, and pleural effusion, it is possible to draw this direct comparison between human and animal cases.

However, the network's inability to concurrently examine orthogonal viewpoints may explain the poor precision with which masses are detected. The high frequency of mass-like features in apparently healthy radiographs is likely to blame for ResNet-50 and DenseNet-121's poor performance in detecting masses. Although the developed EL-DNN had variable State-based evidence, including these components boosts the network's average AUC.

Unfortunately, our study could not include the abovementioned factors due to our limited sample size and the unequal distribution of lesions. It is not always the case that models trained on one piece of data would provide the same results when tested on another data set from a different organization. When utilized for training, data sets collected from many sources improve accuracy. The fact that neither data collection came from a veterinary hospital outside the study's institution is a drawback. Data Set 1 and Data Set 2 were gathered via two distinct radiograph acquisition techniques to account for center generalization. More research is needed to understand further how the proposed EL-DNN performs in conception. Due to the factors above, whether the created EL-DNN has true "in-field" generalization capabilities is yet to be determined. Both general veterinary practitioners and radiology experts stand to benefit in the long run from the developed EL-DNN. Authors believe using deep learning-based technologies in everyday clinical practice will boost efficiency and accuracy. The number of veterinary experts in all fields is far fewer worldwide than those of specialized physicians. Veterinary hospitals are typically smaller than human hospitals. Therefore, general veterinarians must acquire knowledge and skills in many areas of medicine, including imaging, surgery, internal medicine, pathology, etc. The authors believe veterinarians in such a setting would benefit greatly from employing deep learning-based technology to help in clinical practice. Many examples of these algorithms' application to real-world instances involving human patients have been reported and analyzed in the scientific literature. These claims include decreased average reporting latency in a clinical setting and improved diagnostic accuracy of deep learning-based algorithms for identifying pulmonary nodules by experienced radiologists. There has been no assessment of the potential effects of EL-DNN usage in veterinary medicine.

Conclusions

To automate the categorization of canine LL radiographs, a multi-label EL-DNN-based network was built and evaluated. The constructed network's performance on an external test set for detecting radiography findings was inconsistent. Further research is needed to make a network with greater generalization potential, ideally with more radiographs gathered at various veterinary facilities. Furthermore, with a bigger database, VD pictures might be used to assess the network's performance. In the future, EL-DNN-based technologies may help the veterinarian in his daily job, leading to better veterinary care. However, for a victorious deployment of such tools in the medical work stream, the operator must have a thorough understanding of both the benefits and the drawbacks of such technology.

Reference

- [1] Rho, J., Shin, S. M., Jhang, K., Lee, G., Song, K. H., Shin, H., ... & Son, H. Y. (2023). Deep learning-based diagnosis of feline hypertrophic cardiomyopathy. *Plos one*, 18(2), e0280438.
- [2] Yoon, Y., Hwang, T., Choi, H., & Lee, H. (2019). Classification of radiographic lung pattern based on texture analysis and machine learning. *Journal of Veterinary Science*, 20(4).
- [3] Banzato, T., Wodzinski, M., Tauceri, F., Donà, C., Scavazza, F., Müller, H., & Zotti, A. (2021). An AI-based algorithm for the automatic classification of thoracic radiographs in cats. *Frontiers in veterinary science*, 8, 731936.
- [4] Pereira, A. I., Franco-Gonçalo, P., Leite, P., Ribeiro, A., Alves-Pimenta, M. S., Colaço, B., ... & Ginja, M. (2023). Artificial Intelligence in Veterinary Imaging: An Overview. *Veterinary Sciences*, 10(5), 320.
- [5] Celniak, W., Wodziński, M., Jurgas, A., Burti, S., Zotti, A., Atzori, M., ... & Banzato, T. (2023). Inter-species and inter-pathology self-supervised pre-training of deep learning models: a resource to improve the classification of veterinary thoracic radiographs.
- [6] Boissady, E., de La Comble, A., Zhu, X., & Hespel, A. M. (2020). Artificial intelligence evaluating primary thoracic lesions has an overall lower error rate compared to veterinarians or veterinarians in conjunction with the artificial intelligence. *Veterinary Radiology & Ultrasound*, 61(6), 619-627.
- [7] Basran, P. S., & Appleby, R. B. (2022). The unmet potential of artificial intelligence in veterinary medicine. *American Journal of Veterinary Research*, 83(5), 385-392.
- [8] Hennessey, E., DiFazio, M., Hennessey, R., & Cassel, N. (2022). Artificial intelligence in veterinary diagnostic imaging: A literature review. *Veterinary Radiology & Ultrasound*.
- [9] Ott, J., Bruyette, D., Arbuckle, C., Balsz, D., Hecht, S., Shubitz, L., & Baldi, P. (2021). Detecting pulmonary Coccidioidomycosis with deep convolutional neural networks. *Machine Learning with Applications*, 5, 100040.
- [10] Gupta, S., & Blankstein, R. (2021). Detecting Coronary Artery Calcium on Chest Radiographs: Can We Teach an Old Dog New Tricks? *Radiology: Cardiothoracic Imaging*, 3(3), e210123.
- [11] Adrien-Maxence, H., Emilie, B., Alois, D. L. C., Michelle, A., Kate, A., Mylene, A., ... & Federica, M. (2022). Comparison of error rates between four pre trained DenseNet convolutional neural network models and 13 board-certified veterinary radiologists when evaluating 15 labels of canine thoracic radiographs. *Veterinary Radiology & Ultrasound*, 63(4), 456-468.
- [12] Giannasi, C., Rushton, S., Rook, A., Steen, N. V. D., Venier, F., Ward, P., ... & Roberts, E. (2021). Canine thyroid carcinoma prognosis following the utilization of computed tomography-assisted staging. *Veterinary Record*, 189(1), no-no.
- [13] Pinto, I. I. R. (2019). Comparison of Heart Measurements in Thoracic Radiographs Before and After the Treatment of Pulmonary Edema in Dogs with Degenerative Mitral Valve Disease: A Retrospective Study of 18 Clinical Cases (Doctoral dissertation, Universidade de Lisboa (Portugal)).
- [14] Škor, O., Bicanová, L., Wolfesberger, B., Fuchs-Baumgartinger, A., Ruetgen, B., Štěrbová, M., ... & Kleiter, M. (2021). Are B-symptoms more reliable prognostic indicators than substage in canine nodal diffuse large B-cell lymphoma. *Veterinary and Comparative Oncology*, 19(1), 201-208.

- [15] Sukut, S. L., D'Eon, M., Lawson, J., & Mayer, M. N. (2023). Providing comparison normal examples alongside pathologic thoracic radiographic cases can improve veterinary students' ability to identify abnormal findings or diagnose disease. *Veterinary Radiology & Ultrasound*.
- [16] Burti, S., Osti, V. L., Zotti, A., & Banzato, T. (2020). Use of deep learning to detect cardiomegaly on thoracic radiographs in dogs. *The Veterinary Journal*, 262, 105505.
- [17] Li, S., Wang, Z., Visser, L. C., Wisner, E. R., & Cheng, H. (2020). Pilot study: application of artificial intelligence for detecting left atrial enlargement on canine thoracic radiographs. *Veterinary radiology & ultrasound*, 61(6), 611-618.
- [18] Tahghighi, P., Appleby, R. B., Norena, N., Ukwatta, E., & Komeili, A. (2023). Machine learning can appropriately classify the collimation of ventrodorsal and dorsoventral thoracic radiographic images of dogs and cats. *American Journal of Veterinary Research*, 1(aop), 1-8.
- [19] Dumortier, L., Guépin, F., Delignette-Muller, M. L., Boulocher, C., & Grenier, T. (2022). Deep learning in veterinary medicine, an approach based on CNN to detect pulmonary abnormalities from lateral thoracic radiographs in cats. *Scientific Reports*, 12(1), 11418.
- [20] Müller, T. R., Solano, M., & Tsunemi, M. H. (2022). Accuracy of artificial intelligence software for the detection of confirmed pleural effusion in thoracic radiographs in dogs. *Veterinary Radiology & Ultrasound*, 63(5), 573-579.
- [21] Jeong, Y., & Sung, J. (2022). An automated deep learning method and novel cardiac index to detect canine cardiomegaly from simple radiography. *Scientific Reports*, 12(1), 14494.
- [22] Hennessey, R. (2022). Using Machine Learning to Detect Hanging Errors in Canine Thoracic Radiographs.
- [23] Kim, E., Fischetti, A. J., Sreetharan, P., Weltman, J. G., & Fox, P. R. (2022). Comparison of artificial intelligence to the veterinary radiologist's diagnosis of canine cardiogenic pulmonary edema. *Veterinary Radiology & Ultrasound*, 63(3), 292-297.
- [24] Tonima, M. A., Esfahani, F., DeHart, A., & Zhang, Y. (2021, May). A lightweight combinational machine learning algorithm for sorting canine torso radiographs. In 2021 4th IEEE International Conference on Industrial Cyber-Physical Systems (ICPS) (pp. 347-352). IEEE.
- [25] Banzato, T., Wodzinski, M., Burti, S., Vettore, E., Muller, H., & Zotti, A. (2023). An AI-based algorithm for the automatic evaluation of image quality in canine thoracic radiographs.